Article

J. Mex. Chem. Soc. **2014**, *58(2),* 126-136
© 2014, Sociedad Química de México
ISSN 1870-249X

Novel Organo Soluble Polyimides and Polyimide Nanocomposites Based on 1,4-bis((4-aminophenyl)-1,3,4-oxadiazolyl)benzene, BAOB, via BAOB-modified Organoclay

Yagoub Mansoori, and Kamran Darvishi

Department of Applied Chemistry, Faculty of Science, University of Mohaghegh Ardabili, Ardabil, Iran.
ya_mansoori@yahoo.com

Received November 21st, 2013; Accepted January 28th, 2014

Abstract. New, thermally stable polyimides (PI) containing a 1,3,4-oxadiazole ring in the polymer backbone based on 1,4-bis((4-aminophenyl)-1,3,4-oxadiazolyl)benzene, BAOB, were synthesized. The prepared polymers were soluble in polar and aprotic solvents. The obtained results reveal that within the prepared polymers, polyimide **(7)** which has been obtained from BAOB and 4,4'-oxydiphthalic dianhydride, ODPA, has the most improved thermal properties. In the next part, thermally stable organophilic clay was obtained via cation exchange reaction between sodium montmorillonite (Na-MMT) and the hydrochloride salt of BAOB. Then, a series of PI/clay nanocomposite materials (PCNs) were synthesized from the in situ polymerization reaction of BAOB and ODPA via thermal imidization. BAOB-MMT was used as the filler at different concentrations. Intercalation of polymer chains within the organoclay galleries was confirmed by WXRD. The glass transition temperature is increased with respect to pristine PI for PCNs 1-3 wt%. At high clay loadings, the aggregation of organoclay particles results in a decrease in T_g. In the SEM images of the pure polymer too many micro-cracks were observed in the background, while surface homogeneity of PCN 1 wt% is increased and micro-cracks are reduced.
Key words: Polyimide; nanocomposite; Clay modification; montmorillonite.

Resumen. Se sintetizaron nuevas poliimidas térmicamente estables (PI) conteniendo anillos de 1,3,4-oxadiazol en el esqueleto principal, el cual está basado en vencen 1,4-bis ((4-aminofenil)-1,3,4-oxadiazol), BAOB. Los polímeros obtenidos fueron solubles en solventes polares y apróticos. Los resultados obtenidos muestran que de los polímeros sintetizados la poliimida (7) obtenida a partir de BAOB y di-anhídrido 4,4´-oxidiftálico ODPA, obtuvo una mejora en sus propiedades térmicas superior a los demás. En una segunda parte, se obtuvo una arcilla organofílica térmicamente estable vía reacción de intercambio catiónico entre la montmorilonita de sodio (Na-MMT) y la sal de hidrocloruro de BAOB. Las series de materiales de nanocompósitos de PI/arcilla fueron sintetizados por una reacción de polimerización *in situ* de BAOB y ODPA vía imidización térmica. BAOB-MMT fue utilizada como surfactante en diferentes concentraciones. La confirmación de intercalado de las cadenas poliméricas y las galerías de la arcilla fue confirmada por WXRD. La temperatura de transición vítrea del PCNs 1-3% g se incrementó con respecto a la PI original. A altas cargas de arcilla, el fenómeno de agregación de las partículas de arcilla causó una disminución en la Tg. En las imágenes de SEM del polímero inicial, se observa gran cantidad de micro-fracturas, mientras que la homogeneidad de la superficie del PCN 1% g se incrementa y las micro-fracturas disminuyen.
Palabras clave: Poliimidas; Nanocompósito; Modificación de Arcilla; Montmorilonita.

Introduction

Aromatic polyimides are the most useful super engineering plastics and have been applied widely in the areas of modern industries [1-2]. They have found their way into biochip design [3], aerospace [4-5], optoelectronic applications [6], gas separation [7-8], coating [9], superhydrophobic surfaces [10], photocatalyst for hydrogen generation[11] and composites [12-13].

Composition of inorganic materials with organic polymers has been receiving increasing research attention during recent decades. It has been well-known that dispersion of small portions of inorganic clay in a polymer matrix significantly improves the physical and chemical properties when compared with virgin polymers or conventional composites. These improvements can include solvent resistance [14], ionic conductivity [15], enhanced fire retardance [16], increased corrosion protection [17], increased strength and heat resistance [18], decreased gas permeability [19], high moduli [20-21], and dielectric properties [22]. Clay is a layered silicate, and the most commonly used clay in the preparation of polymer/clay nanocomposites (PCNs) is montmorillonite (MMT). The chemical structure of MMT consists of two fused silica tetrahedral sheets sandwich an edge-shared octahedral sheet of either magnesium or aluminum hydroxide [23]. The Na^+ and Ca^{2+} ions adsorbed in the interlayer region are exchangeable with organic cations such as long chain alkyl ammonium and alkylphosphonium ions [24-25]. The improvements in thermal and mechanical properties of polymer/clay nanocomposites (PCNs) are due to the lamellar structure of MMT results in high in-plane strength and stiffness, and a high aspect ratio [26-27]. Nanostructured hybrid materials also show wide potential applications in various areas such as in coatings [28], catalysis [29] and biotechnology [30], shape memory polymers [8], and fuel cells [9].

Using regular commercial organoclays as compatibilizer may be suitable for polymer blends prepared with a low processing temperature. These organoclays modified with alkyl ammonium surfactants have low thermal stability and start to decompose around 200 °C, whereas the melt-processing temperatures of most polymers are typically above 200 °C [31]. Furthermore, the preparation and processing of PI/clay nanocomposites is carried out at high temperatures, and the thermal decomposition of the long carbon chain of quaternary

ammonium salts is inevitable. Thermal decomposition during processing can initiate/catalyze polymer degradation, in addition to a variety of undesirable effects during processing and in the final product [32-35]. To avoid the detrimental effects of the lower thermal stability of alkyl ammonium treated clays, modification of clay minerals with imidazolium [36] and phosphonium [37] salts have been noted. As another approach, using of aromatic amines and diamines, as swelling agents, has also been considered in the preparation of polyamide and polyimide (PI) nanocomposites. Using the same diamine monomer with an organic modifier can improve the miscibility between the organics-modified silicate layers and the poly (amic acid), increasing the probability of a reaction between the organoclay and the poly (amic acid). Tyan et al. reported the synthesis of 4,4'-oxydianiline (ODA) modified clay. They prepared clay-polyimide nanocomposites from the polymerization reaction of ODA with 3,3',4,4'-benzophenonetetracarboxylic dianhydride (BTDA) via ODA-modified clay [38]. Yeh et al. used ODA-modified clay for the preparation of PI/clay nanocomposites obtained from 4,4'-oxydiphthalic anhydride (ODPA) and 1,4-bis(4-aminophenoxy)-2-*tert*-butylbenzene (BATB) polyimide. The dispersal of MMT clay platelets into the PI matrix was found to boost the thermal stability. The incorporation of clay platelets into the PI membrane resulted in an enhancement of O_2 and H_2O molecular barrier properties [32]. Huang et al. recently reported the preparation of high performance PI/clay nanocomposite materials based on a dual intercalating agent system. They applied hexadecyltrimethylammoniumbromide-4,4'-oxydianiline for MMT treatment. All PCN materials containing dual intercalating agent-modified MMT clay exhibited enhanced thermal, mechanical and gas barrier properties [27].

It has been shown that, the thermal stability of polymers can be raised by the incorporation of 1,3,4-oxadiazole moieties into the polymer structure [39]. Aromatic poly(1,3,4-oxadiazole)s are a class of heterocyclic polymers possessing chemical and thermal stability. These polymers are classified as high-performance polymers with excellent mechanical strength and stiffness. The outstanding thermal stability is ascribed to the electronic equivalency of the oxadiazole ring to the phenylene ring structure, which has high thermal-resistance [40]. These features cause polymers containing 1,3,4-oxadiazole moieties to act as alternatives in the development of heat flame-resistant, semi-conducting, fiber-forming and thermally stable membranes for gas separation [41]. The synthesis and morphological characteristics of 1,3,4-oxadiazole containing polyimide/TiO_2 nano hybrid films have been reported by Chiang et al. [42].

Recently, our research team successfully carried out the synthesis of 2-(5-(3,5-diaminophenyl)-1,3,4-oxadiazole-2-yl)pyridine, POBD, which contains an oxadiazole moiety, Scheme 1. POBD has been used for the preparation of new thermally stable poly(amide-imide)s [43], polyamides [44], polyimides [45], and polyimide/Cloisite 20A nanocomposites [13]. It was also used as a swelling agent for the modification of sodium montmorillonite. The modified organoclay was used in the preparation of polyimide/organoclay hybrid films with BTDA [12].

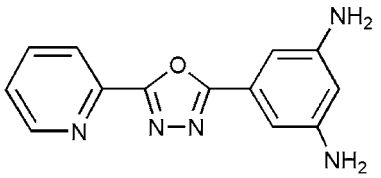

Scheme 1 Chemical structure of POBD.

In this work, BAOB **(4)**, another 1,3,4-oxadiazole containing diamine, was synthesized according to the method described in the literature [46]. It was then reacted with aromatic dianhydrides to give the corresponding new thermally stable polyimides after thermal imidization of their corresponding poly(amic acid) intermediate. The polymers were characterized by spectroscopic methods and elemental analysis (CHN). Based on the thermal properties, polyimide **(7)** which has been obtained from BAOB and ODPA was selected for the preparation of PI/clay nanocomposite materials. The dihydrochloride salt of BAOB was used as a swelling agent for the modification of sodium montmorillonite. The novel modified organoclay (BAOB-MMT) was used in the preparation of PI/organoclay hybrid films with ODPA. The thermal stability of BAOB is higher than those for commonly used quaternary alkyl ammonium salts. Therefore, thermal degradation will be prevented during heat treatment needed for curing of poly (amic acid)s. The obtained films were studied by FT-IR spectroscopy, WXRD, and SEM. The thermal properties were examined by TGA and DSC.

Experimental

Instruments

NMR spectra were obtained on a Bruker 300 MHz spectrophotometer. The FT-IR (KBr) spectra were recorded on a PerkinElmer RXI spectrophotometer (2 w/w% in KBr, resolution 4 cm^{-1}, scan no. 6). Thermal analysis (TGA-DTA) and differential scanning calorimetry (DSC) were carried out on a Linseis STA PT 1000 and a DSC PL instruments (nitrogen atmosphere, scan rate 10 °C/min), respectively. DSC measurements were performed after heating the polymer samples to 150 °C and then cooling to room temperature; this removed any adsorbed water on the polymer. Elemental analyses of the samples were performed on an Elemental Vario TEL instrument. Inherent viscosities were measured by an Ostwald viscometer at 25 °C in DMF. The mass spectrum (electron impact, 70 eV) was obtained on an Agilent Technologies 5973Network MSD mass spectrometer. Wide-angle X-ray diffraction (WXRD) measurements were performed at room temperature on a Simence D500 X-ray diffractometer (Germany) using Ni-filtered Cu-K_α radiation. The scanning rate was 1°/min over a range of 2θ = 2-10°. Scanning Electron Microphotographs (SEM) were obtained on a LEO 1430VP instrument.

Materials

Commercial sodium montmorillonite was purchased from Southern Clay Products (Gonzales, TX). 4,4'-Oxydiphthalic anhydride (ODPA) were purchased from Aldrich and used as received. N,N'-dimethylacetamide (DMAc) and N,N-dimethylforamide (DMF) were obtained from Merck and dried over sodium hydride.

Terephthalic dihydrazide
Dimethyl terephthalate (2.000 g, 10.31 mmol) was dissolved in 50 mL methanol and hydrazine monohydrate (5 mL, 100 mmol) was added. The reaction mixture was refluxed for 24 h. After cooling to room temperature, the precipitate was filtered, washed with water thoroughly and dried in vacuum to give 1.890 g white powder (Yield: 94.5%, mp > 300 °C). FT-IR (KBr): ν cm^{-1}: 3326 (s), 3213 (m), 3036 (m), 1696 (m), 1629 (s), 1542 (s), 1490 (s), 1341 (s), 929 (s).

1,4-Bis((4-aminophenyl)1,3,4-oxadiazolyl)benzene, BAOB (4)
The compound was synthesized according to the literature [46]. A mixture of terephthalic dihydrazide (0.194 g, 1 mmol) and *p*-aminobenzoic acid (0.274 g, 2 mmol) in trifluoroacetic acid (10 mL) was refluxed for 4-6 h. The reaction mixture was slowly poured over crushed ice and kept overnight. The solid thus separated out was neutralized with $NaHCO_3$, filtered, washed with water and then re-crystallized from ethanol to give 0.253 g brown powder. (Yield = 45.3%, m.p. = 283-286 °C). FT-IR (KBr, cm^{-1}): 3325 (m), 3218 (m), 1608 (s), 1497 (s), 1443 (m), 1394 (w), 1313 (m). ^{13}C NMR (75 MHz, DMSO-d_6, Δ, ppm): 165.1, 164.8, 152.6, 129.3, 128.3, 127.9, 127.1, 126.2, 113.5, 109.4. ^{1}H NMR (300 MHz, DMSO-d_6, Δ, ppm): 6.0 (s), 6.7 (d, J = 8.2), 7.8 (d, J = 8.3), 8.0-8.3 (m). ^{1}H NMR (DMSO-d_6, D_2O): (ppm): 6.7 (d, J = 7.8), 7.7 (d, J = 8.2), 7.9-8.2 (m). $(m/e)^+$: 396 (0.23%).

General procedure for the preparation of polyimide films (5-9)
To a solution of BAOB (0.495 g, 1.25 mmol) in 5 ml of DMAc, was added gradually bis-anhydride (1.25 mmol). The mixture was stirred at room temperature for 2 h under argon. The obtained DMAc solution of poly(amic acid) was poured onto a glass plate, allowed to stand at room temperature overnight, and then heated from 60 to 270 °C (at a heating rate of 1 °C/min) in a furnace. The film was then peeled off from the glass plate to obtain the PI film.

Preparation of the organophilic clays BAOB-MMT

Sodium montmorillonite (2.000 g) was stirred in 100 ml of distilled water (beaker A) at room temperature overnight. A separate solution containing BAOB (0.9152 g, 2.308 mmol) in 200 ml of distilled water (beaker B) was kept under magnetic stirring at 80 °C and then 35% aqueous HCl was added to adjust the pH value to about 3-4. After complete dissolution of diamine and stirring for additional 1 h, the contents of beaker A were added at approximately 10 ml/min under vigorous stirring and then stirred at 80 °C for an hour. The organoclay was filtered in a Buchner funnel. To remove any excess of ammonium ions, the precipitate was washed with distilled water until a chloride ion test with a 0.1 M $AgNO_3$ solution was negative and then dried in vacuum at 50 °C for 48 h [47].

Preparation of the PI/clay hybrid film
A poly(amic acid)/clay dispersion was prepared according to method II described by Gu et al. [48]. A typical procedure to prepare a N,N-dimethylacetamide (DMAc) solution of poly(amic acid)/clay containing 1 wt% clay is described as follows: organophilic clay (0.090 g) was magnetically stirred vigorously at room temperature for 24 h in 3 ml of DMAc to yield a DMAc dispersion of MMT (beaker A). A separate solution was prepared by dissolving BAOB (0.496 g, 1.25 mmol) in 2 ml of DMAc under magnetic stirring for 10 min at room temperature (beaker B). The contents of the beaker B were added to beaker A and stirred vigorously for another 24 h at room temperature. Then, a solution of ODPA (0.388 g, 1.25 mmol) in 2 ml of DMAc was prepared under magnetic stirring for 10 min at room temperature (beaker C). Beaker C was then added to beaker A+B and the contents were stirred for an additional 24 h at room temperature to yield a DMAc solution of poly(amic acid). The obtained DMAc solution of poly(amic acid)/clay was poured on a glass plate, allowed to stand at room temperature overnight, and then heated from 60 to 270 °C (at a heating rate of 1 °C/min) in a high temperature oven. The film was then peeled off from the glass plate to obtain the PI/clay hybrid film.

Results and Discussions

Monomer and polymer synthesis

The diamine BAOB **(4)** was obtained in two steps according to the literature reported method [46] starting from dimethylterephthalate **(1)**. Terephthalic dihydrazide **(2)** was obtained upon treatment of dimethylterephthalate with hydrazinehydrate in refluxing MeOH. The subsequent cyclocondensation reaction of dihydrazide derivative **(2)** with two folds of *p*-aminobenzoic acid **(3)** in trifluoroacetic acid gave BAOB **(4)** in overall 42.8% yield, (Scheme 2).

The chemical structures of BAOB were confirmed by FT-IR, ^{1}H NMR, ^{13}C NMR and mass spectroscopy techniques.

Poly(amic acid)s are requisite intermediate polymers for preparing polyimides and polyimide nanocomposites [2]. In this work, BAOB **(4)** was reacted with aromatic dianhydrides in DMAc at room temperature to give the corresponding poly(amic acid)s. Polyimide films (**5**-**9**) were obtained via thermal imidization of poly(amic acid) solutions, (Scheme 3).

The IR spectrum of the poly(amic acid) sample (Fig. 1a) shows absorption bands at 1852 cm^{-1}, and 1610 cm^{-1} which relate to C=O and -C=N- stretching vibration of the oxadiazole ring, respectively. The IR absorptions occurring at approxi-

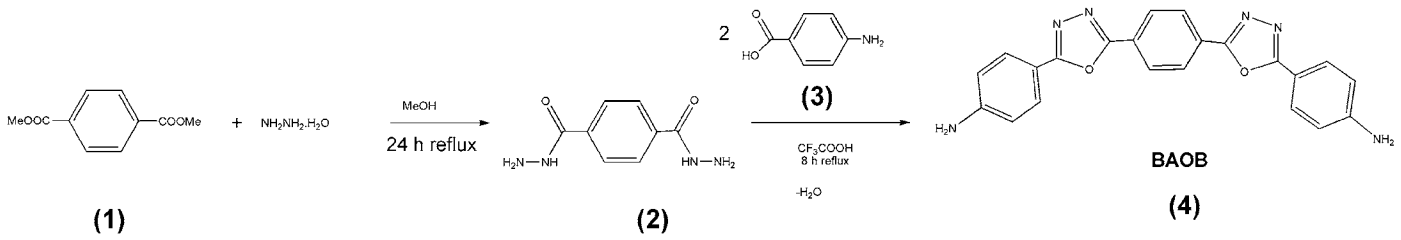

Scheme 2 Synthesis of 1,4-bis[(4-aminophenyl)-1,3,4-oxadiazolyl] benzene (BAOB).

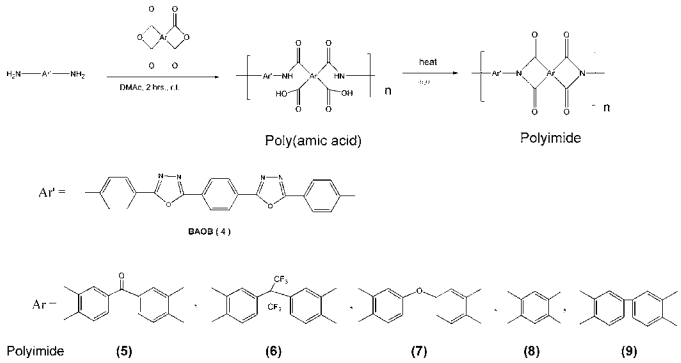

Scheme 3 Synthesis of polyimides using BAOB**.**

mately 1778, 1728, 1358, 1077, and 710 cm^{-1} determined the presence of imide functional groups in the PI film (Fig. 1b).

The conversion from poly(amic acid) to polyimide was confirmed by the presence of these strong imide absorption bands and the absence of a broad absorption band due to the amino (N-H) and hydroxyl (OH) groups [49]. Infrared spectroscopy data, inherent viscosities, and reaction yields are listed in Table 1.

Solubility test results (Table 2) showed that the obtained polyimides are soluble in concentrated sulfuric acid and polar, aprotic solvents such as DMSO, DMAc, DMF, and NMP at both ambient and elevated temperatures. They are insoluble in polar, protic and less polar solvents. For this experiment, about 0.01 g of the polymer sample was examined in 1 mL of the solvent at room temperature and at boiling temperature.

The inherent viscosities of the polyimide solutions were in the range of 0.20-0.32 dL/g (measured in DMF with a concentration of 0.125 dL/g at 25 ± 0.5 °C). The highest viscosity was noted with polyimide **(8)**, obtained from the reaction of BAOB **(4)** with pyromellitic dianhydride.

The elemental analysis (CHN) data are presented in Table 3. The calculated and found values for the CHN analyses agreed.

Thermal analysis results of the polymers are summarized in Table 4. TGA, DSC, and DTA were used to study the thermal behaviors of the obtained polyimides. Clear melting endotherms observed without any thermal decomposition for the polyimides **(5)** and **(7)**. Based on DTA measurement, the glass transition temperature was occurred at 295 °C for polyimide **(5)**, which was obtained from BAOB and BTDA. For this poly-

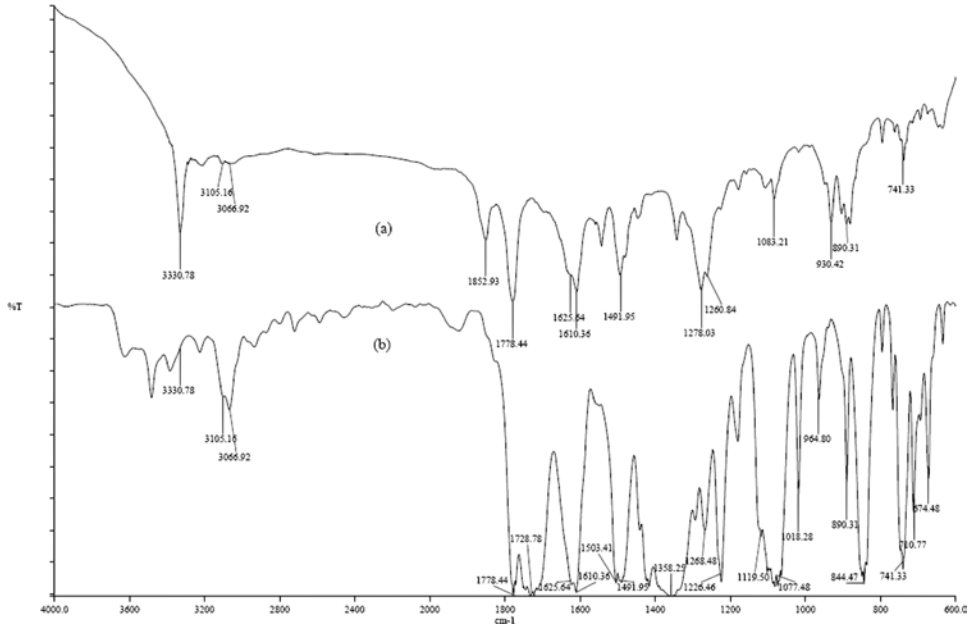

Fig. 1 FTIR spectra of a) poly(amic acid) (KBr) and b) polyimide (Film).

Table 1. Infrared spectroscopy, inherent viscosity results, and yields of the polyimides.

Polymer	IR data (cm^{-1})	Inherent Viscosity	Yields (%)
		η_{Inh} (dL/g)[a]	
5	3110 (w)[b], 3074 (w), 1779 (s)[c], 1720 (br [d], s), 1609 (s), 1499 (s), 1346 (s), 1082 (s), 851 (s)	0.20	66.4
6	3116 (w), 3080 (w), 1785 (m)[e], 1728 (s), 1612 (m), 1499 (s), 1370 (s), 842 (m)	0.22	71.3
7	3105 (w), 3069 (w), 1779 (s), 1725 (br; s), 1610 (s), 1493 (s), 1356 (br; s), 844 (s)	0.25	54.4
8	3105 (w), 3045 (w), 1776 (m), 1725 (br, s), 1606 (s), 1499 (s), 1367 (s), 825 (m)	0.32	55.3
9	3093 (w), 3069 (w), 1782 (m), 1746 (s), 1612 (m), 1496 (m), 1367 (s), 844 (m)	0.25	57.8

[a] Measured in DMF with a concentration of 0.125 g/dL at 25 ± 0.5 °C.
[b] Peak with weak intensity.
[c] Peak with strong intensity.
[d] Broad peak.
[e] Peak with medium intensity.

Table 2. Solubility of the prepared polyimides in common organic solvents.

Polymer	5		6		7		8		9	
Solvent	Δ	R.T.	Δ	R.T.	Δ	R.T.	Δ	R.T.	Δ	R.T.
DMSO	++	++	++	++	++	++	++	++	++	++
DMF	++	++	++	++	++	++	++	++	++	++
DMAc	++	++	++	++	++	++	++	++	++	++
NMP	++	++	++	++	++	++	++	++	++	++
MeOH	—	—	—	—	—	—	—	—	—	—
$CHCl_3$	—	—	—	—	—	—	—	—	—	—
Acetone	—	—	—	—	—	—	—	—	—	—
H_2SO_4	++	++	++	++	++	++	++	++	++	++

++ Soluble.
−+ Low solubility.
— Insoluble.

Table 3. Elemental analysis of the polyimides**.**

Polymer	Compnd. St.	Calcd.			Found		
		%C	%H	%N	%C	%H	%N
5	$(C_{39}H_{18}N_6O_7)_n$	68.62	2.66	12.31	69.52	2.56	11.34
6	$(C_{41}H_{18}F_6N_6O_6)_n$	61.20	2.25	10.44	61.96	2.11	9.27
7	$(C_{38}H_{18}N_6O_7)_n$	68.06	2.71	12.53	68.22	2.57	12.03
8	$(C_{32}H_{14}N_6O_6)_n$	66.44	2.44	14.53	66.64	2.37	13.81
9	$(C_{38}H_{18}N_6O_6)_n$	69.72	2.77	12.84	69.13	2.87	11.45

mer, the T_g value was not observed by DSC measurement. This may be due to overlapping of T_g and melting endotherms (T_m = 299.7, measured by DSC). Polyimide **(7)**, which was obtained from BAOB and ODPA, showed the glass temperature at 262.2 °C and 249 °C, measured by DSC and DTA methods, respectively. The relatively low T_g of polyimide **(7)** can be attributed to the presence of flexible ether linkages in the polymer main chain.

The TGA curves of prepared polyimides are shown in Fig. 2 and the results are summarized in Table 4. As seen, the temperature for 10% weight loss **(**$T_{10\%}$) and the initial decomposition temperature (T_D) of polyimides **(5)** (T_{10} =511.1 °C, T_D = 475.1 °C) and **(7)** ($T_{10\%}$ =504.2 °C, T_D = 476.8 °C) are close to each other and higher than those for other polyimides. Char yields at 574 °C are also high for the polyimides **(5)** and **(7)** in compared with other prepared polyimides. Based on the obtained results from DSC, DTA, and TGA measurements and observing T_g for the polyimide **(7)**, it can be conclude that among the prepared polymers, polyimide **(7)** has the most improved thermal properties. Therefore this polymer was chosen for the preparation of PCN materials.

Table 4. Thermal properties of the polyimide films.

Polymer	T_g (°C) [a]	T_m (°C) [a]	10% weight loss (°C)	T_D (°C)[b]	Char Yield [c]
5	N.O. [d] (295)	299.7 (N.O.)	511.1	475.1	77.0
6	N.A. [e] (274)	N.A. (295.5)	436.3	391.4	63.5
7	262.2 (249)	304.7 (N.O.)	504.2	476.8	73.1
8	N.A. (278)	N.A. (N.O.)	405.1	367.7	56.9
9	N.A. (292)	N.A. (348.8)	385.6	356.0	57.7

[a] Obtained based on DSC measurements. The values in the parentheses obtained based on DTA measurements.
[b] Onset decomposition temperature.
[c] At 574 °C.
[d] Not observed. Glass transition temperature tentatively overlapped with melting enotherm.
[e] Not analyzed.

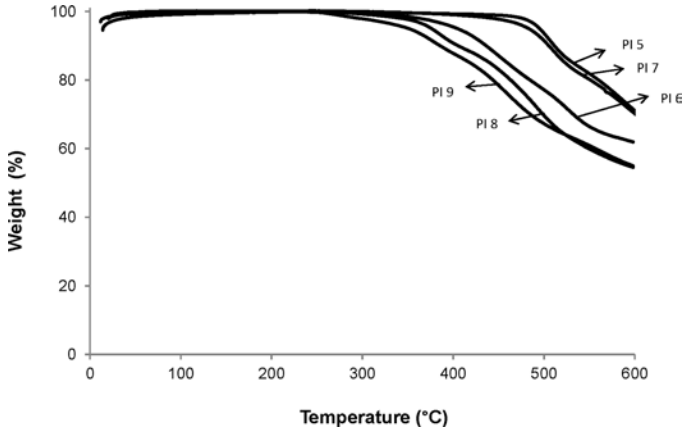

Fig. 2 TGA curves (nitrogen atmosphere, scan rate 10 °C/min) of the polyimides.

Preparation and characterization of BAOB-modified organoclay

Organophilic clay was prepared by a typical cation exchange reaction between the sodium cations of Na-MMT clay and the ammonium ions of the intercalating agent, BAOB. Scheme 4 presents a schematic drawing of the modification step.

Fig. 3 shows FT-IR spectra of BAOB, sodium montmorillonite, and BAOB-modified organoclay. The spectrum of organoclay exhibits the characteristic bands of MMT and BAOB: N-H stretching at 3214 cm^{-1}, C-N stretching vibration of the aromatic ring at 1635 cm^{-1}, -C=N- stretching vibration of the oxadiazole ring at 1610 cm^{-1}, and -C-O- stretching vibration of oxadiazole ring at 1442 and 1499 cm^{-1}.

Fig. 4 presents the X-ray diffraction patterns of organoclay and pristine clay. A strong peak is observed at $2\theta = 8.76°$ for sodium montmorillonite, corresponding to the (001) plane, indicating that the interlayer spacing (d_{001}-spacing) of the clay is about 1.0 nm. The WXRD peak for BAOB-modified clay is observed at $2\theta = 6.70°$, which corresponds to an interlayer d_{001}-spacing of 1.3 nm. The replacement of sodium ions with the ammonium ions of BAOB seems to increase the basal spacing of layered silicate.

The thermal treatment of sodium montmorillonite under nitrogen consists of two main stages. In the first stage, from ambient temperature to 200 °C, free water molecules physically adsorbed on the external surfaces of crystals are removed, along with the hydrating water molecules around the exchangeable cation located inside the interlayer space. The second stage is attributed to the dehydroxylation of the structural silanol units of the montmorillonite in the range of 500-1000 °C. The temperature intervals of dehydration corresponding to these processes as well as the amount of water released depends on the nature of adsorbed cations and the hydration of the surface. On the other hand, organically modified montmorillonite un-

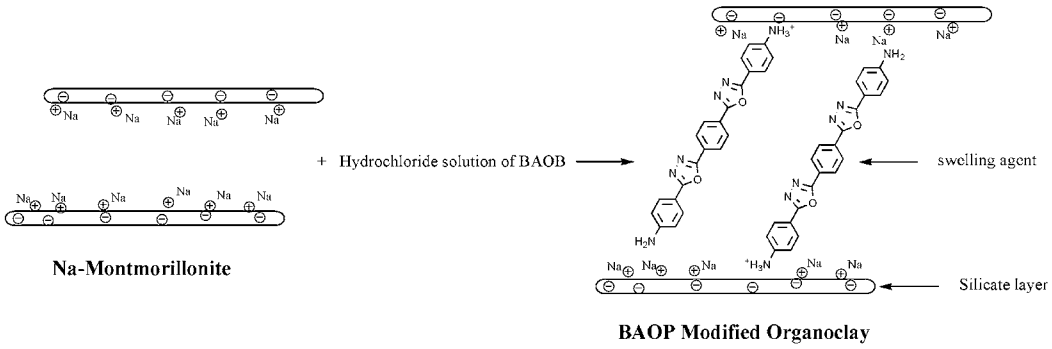

Scheme 4 Modification of sodium montmorillonite with BAOB.

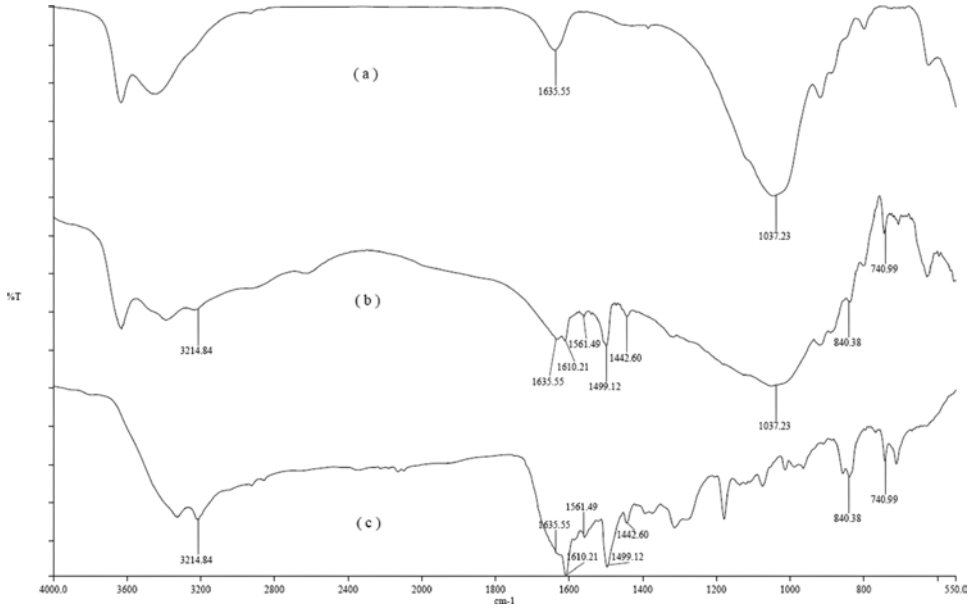

Fig. 3 IR spectrum of: a) sodium montmorillonite, b) BAOB-modified sodium montmorillonite, and c) BAOB.

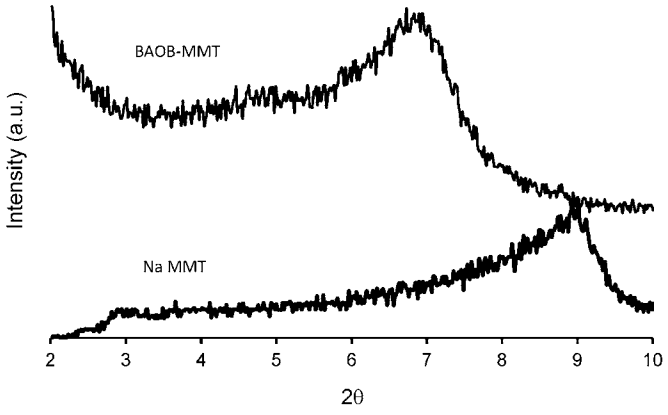

Fig. 4 X-Ray diffraction patterns of Na-MMT and BAOB-MMT.

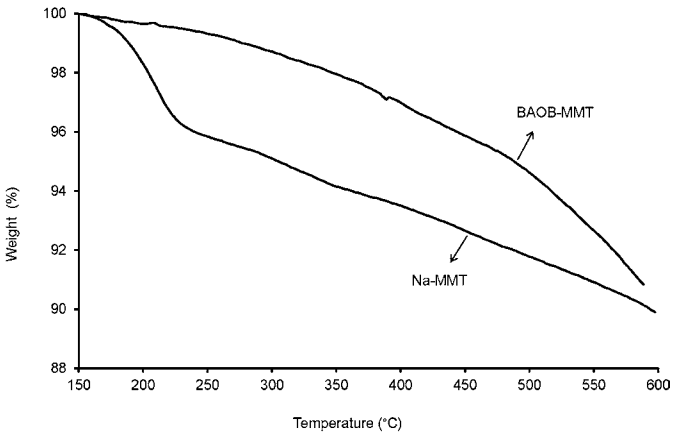

Fig. 5 TGA curves (N_2 atmosphere, scan rate of 10 °C/min) of Na-MMT and BAOB-MMT.

dergoes a four-step decomposition process. The vaporization of free water takes place at temperatures below 200 °C, while the surfactant's decomposition occurs in the temperature range of 200-500 °C. Dehydroxylation of the aluminosilicates occurs between 500-800 °C. The last step is the decomposition associated with the combustion reaction between organic carbon and inorganic oxygen [50]. Fig. 5 shows the TGA curves of the Na-MMT and the BAOB-modified organoclay.

Pristine Na-MMT contains a large quantity of water due to the intercalation of hydrated sodium (Na^+) and hydrated calcium (Ca^{2+}) cations inside the clay layers (Table 5). The clay undergoes a 4.16% weight loss in the range from ambient temperature to 250 °C. BAOB- treated Na-MMT shows only 0.68% weight loss within the mentioned temperature range. The presence of the aromatic ammonium ion within the interlayer spacing lowers the surface energy of the inorganic material and transforms the hydrophilic silicate surface to an organophilic one. In the BAOB-modified organoclay, the thermal decomposition of the surfactant molecules starts at about 250 °C. This temperature is higher than the decomposition temperature of montmorillonite modified with aliphatic long chain surfactants, which occurs below 200 °C [33]. This study suggests that the BAOB-modified organoclay can be used in

Table 5. Thermal properties of Na-MMT and BAOB-modified organoclay.

Clay	T_D (°C)[a]	5% weight loss (°C)	Char Yield [b]
Na-MMT	—	303.8	90.23
BAOB-MMT	250	487.3	90.10

[a] Onset decomposition temperature.
[b] At 585 °C.

the preparation of PI nanocomposites that need to be cured at elevated temperatures.

The amount of loaded diamine can be estimated by TGA measurement. The organophilic clay undergoes an 8.46% weight loss in the temperature range of 250-588 °C, while under the same condition Na-MMT shows only 5.69% weight loss. The difference between weight losses of Na-MMT and BAOB-MMT (Δm = 2.77%) can be attributed to the weight of the loaded diamine. Therefore, the amount of loaded diamines (27.7 mg/g of clay) can be calculated from Eq. (1).

Scanning Electron Microscopy (SEM) demonstrates significant changes on the surface of the BAOB-modified organoclay. The sodium montmorillonite particles seem to be stuck together due to moisture (Fig. 6a-b), but the organically modified clay particles are relatively separated (Fig. 6c,d). The modification reaction seems to reduce the hydrophilicity of the clay. This study is in accordance with TGA results.

Preparation and characterization of PI/clay nanocomposite materials (PCNs)

The preparation and characterization of polyimide nanocomposite materials with different contents of BAOB-modified organoclay are also investigated. Scheme 5 shows a procedure for the preparation of PI/clay nanocomposites by thermal imidization according to method II reported by Gu et al. [48].

An appropriate amount of BAOB-modified organoclay was introduced into DMAc and stirred magnetically for 24 h at room temperature. A BAOB solution in DMAc was added to this suspension and stirred for an additional 24 h at room temperature under argon. The ODPA solution in DMAc was then added to this mixture and stirred vigorously for another 24 h at room temperature to give a DMAc solution of poly(amic acid)/clay. The resulting solution was then poured onto a glass plate, left at room temperature overnight, and then heat treated in a high temperature oven from 60 to 300 °C (at a heating rate of 1 °C/min).

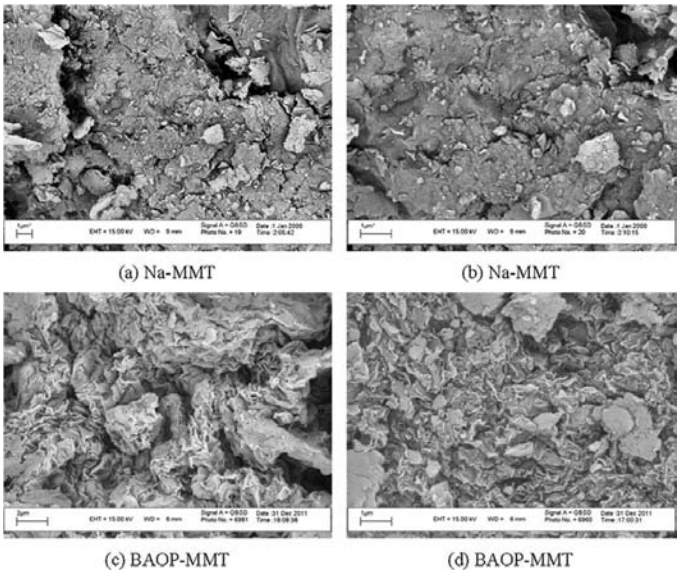

Fig. 6 SEM images of Na-MMT at a) 15000x and b) 30000x, and of BAOB-MMT at c) 15000x and d) 30000x magnifications.

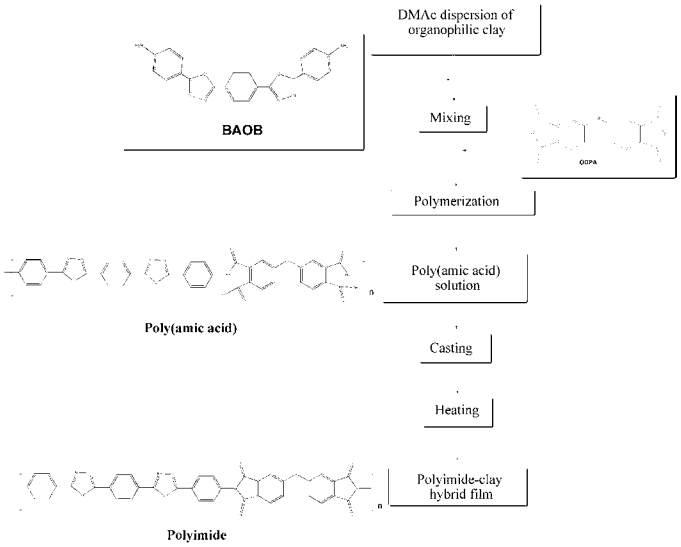

Scheme 5 Preparation of PCN materials by thermal imidization.

Fig. 7 presents X-ray diffraction patterns of Na-MMT, BAOB-modified organoclay, and PI hybrid films with various organoclay contents. The interlayer d_{001}-spacing can be calculated from peak positions using Bragg's law: $n\lambda = 2d \sin \theta$, where λ is the X-ray wavelength (1.5418 Å). The d_{001}-spacing of Na-MMT was measured as 1.0 nm ($2\theta = 8.76°$). In general, a larger interlayer spacing should assist the intercalation of the polymer chains. It should also lead to easier dissociation of the clay, which should result in hybrids with better clay dispersion. A strong peak appears at $2\theta = 6.70°$ ($d = 1.3$ nm) representing the diffraction from the d_{001} crystal surface of the BAOB-MMT. The X-ray diffraction pattern of PCN 1% does not show any diffraction peak, indicating that the silicate layers of organoclay have been either intercalated to a distance of more than 4.4 nm ($2\theta < 2.0°$) or completely exfoliated. This observation reveals

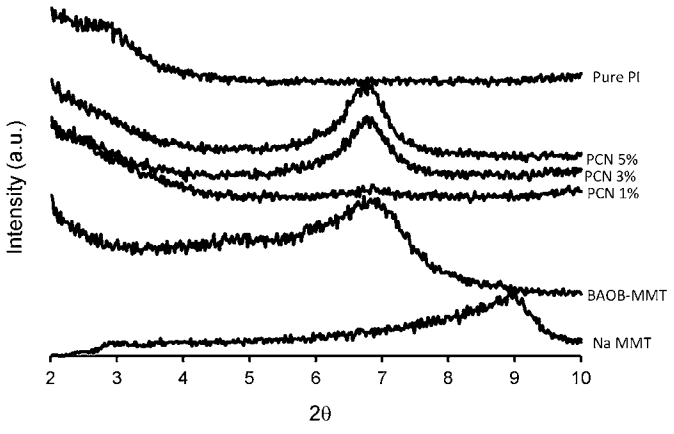

Fig. 7 Wide-angle powder X-ray diffraction patterns of BAOB-MMT, PI, and PI/clay nanocomposites.

that the organophilic clay in this hybrid disperses homogeneously into the polyimide matrix. This homogeneous dispersion may be due to the existence of some physicochemical interactions between the polyimide and the organophilic clays. The absence of any diffraction peak between 2 and 10° is also observed for pure polyimide. Polyimide/clay nanocomposites 3-5% show a broad diffraction peak at 6.75-6.77° (d = 1.3 nm). In a very extensive study, Connell et al. proved that in the polyimide hybrids, the observation of this peak is the consequence of the thermal decomposition of the organic surfactant. This phenomenon leads to collapsing of the clay layers that reduces the d_{001}-spacing and the formation of collapsed agglomerated structure. The clay agglomerates apparently retained their original structure, and it is doubtful that they were impregnated by monomer prior to polymerization [51]. Therefore, both intercalated/exfoliated and agglomerated structures are present in the nanocomposite with clay content higher than 1%.

A substantial increase in the intensities of the WXRD peak was observed for the PCNs of loading up to 5 wt%, which suggests that the dispersion is better at a lower clay loading than at a higher clay loading. This observation also implies that there is no significant quantity of intercalated/exfoliated organoclay in the nanocomposites with high clay content, and the organoclay is mainly present in the form of collapsed agglomerated form. The WXRD data are summarized in Table 6.

Table 7 summarizes the results of thermal analyses by TGA and DSC for PI and PCNs. As seen, the T_g value increases dramatically from 262.2 °C for pure polyimide to 300.2 °C for PCN 3% wt%. The melting endotherm did not also observe for PCN 1 and 3 wt%. This is tentatively attributed to the confinement of the intercalated polymer chains within the clay galleries that prevent the segmental motions of the polymer chains [17]. However, further addition of organoclay up to 5 wt% leads to a decrease in T_g. This decrease might be due to the aggregation of organoclay particles that reduces the interfacial interaction between organoclay and the PI matrix [23]. Furthermore, the melting endotherm of PCN 5 wt% observes at 297.2 °C that is very close to the melting temperature of the virgin polymer. This indicates phase separation as a result of organoclay coagulation at high clay loadings.

Fig. 8 shows TGA curves of the pure polyimide and nanocomposites with 1-5 wt% clay loadings. As seen, temperature of 10% weight loss and char yield at 574 °C are not significantly influenced by amount of clay loading for PCNs 0-3 wt%. However, thermal properties of PCN 5 wt% are dramatically improved. The improvement of thermal stability can be attributed to the barrier effect of organoclay. BAOB-MMT is a layered structure and small molecules generated during thermal decomposition process cannot permeate, and thus have to bypass, organoclay layers [52].

Scanning electron microscopy (SEM) was used to consider the morphology of the polymer and nanocomposite film surfaces. Some significant and interesting changes have been observed in the PCN 1 wt% surface with respect to virgin PI film, Figs. 9a-d. Too many micro-cracks are observed in the background of pure polyimide surface. However, as can be seen in the pictures, homogeneity along with the continuation of the film surface is increased in the PCN 1wt%.

Table 6. Diffraction peaks and basal spacing of Na-MMT, BAOB-MMT, the polyimide, and PI/clay nanocomposites**.**

Product	Diffraction peak and basal spacing	
	Typical diffraction peak (°)	Basal spacing (nm)
Na-MMT	8.76	1.0
BAOB-MMT	6.70	1.3
Pure Polyimide	—	—
[a] PCN 1%	—	—
PCN 3%	6.77	1.3
PCN 5%	6.75	1.3

[a] Polymer-clay nanocomposites.

Table 7. Thermal properties of the polyimides.

Polymer	T_g(°C)[a]	T_m(°C)[a]	10% weight loss (°C)	T_D (°C)[b]	Char Yield[c]
Pure Polyimide **(7)**	262.2	304.7	504.2	476.8	73.1
PCN 1%	296.8	—	499.9	472.4	70.3
PCN 3%	300.2	—	496.5	472.8	72.2
PCN 5%	266.7	297.2	543.3	498.1	73.0

[a] Obtained based on DSC measurements.
[b] Onset decomposition temperature.
[c] At 574 °C.

Conclusions

New, thermally stable polyimides and containing 1,3,4-oxadiazole ring in the main chain based on BAOB **(4)** were synthesized. Solubility tests showed the polymers to be soluble in polar and aprotic solvents such as DMF, DMSO, NMP, and

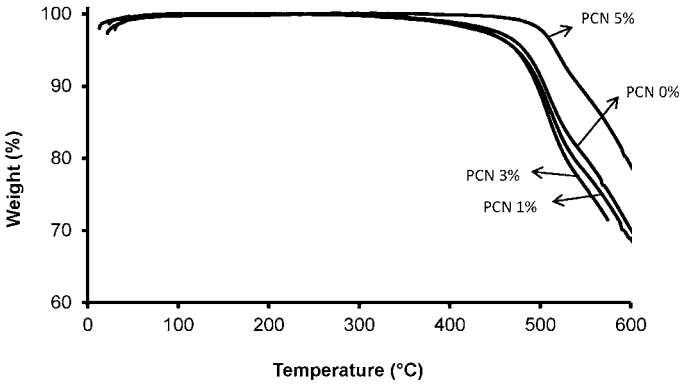

Fig. 8. TGA Curves of PI and PI/clay nanocomposites with various organoclay contents.

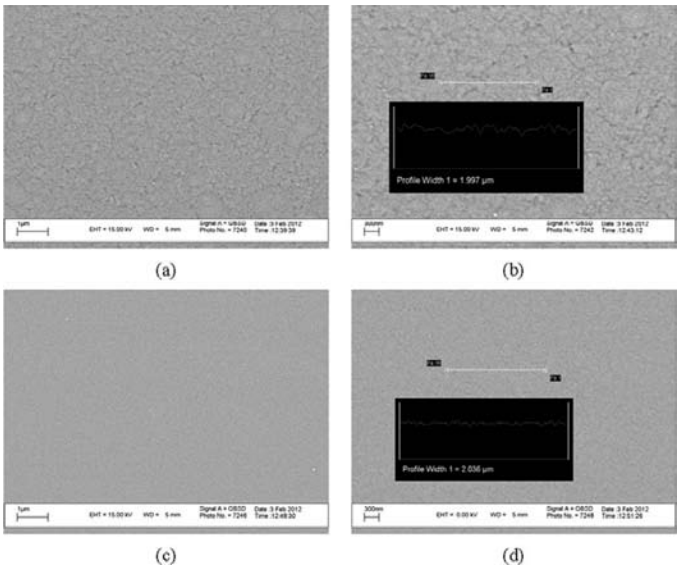

Fig. 9 SEM images of the films obtained from PI (a) at 30000x and (b) at 50000x, and PCN 1% (c) at 30000x and (d) at 50000x.

DMAc. The thermal behaviours of the polymers were studied by TGA, DTA and DSC methods. Softening temperatures were observed for all polymers except for polyimides **(8)**, which it was obtained from BAOB and pyromellitic dianhydride. DSC, DTA, and TGA measurements showed among the prepared PIs, polyimide **(7)** has the most improved thermal properties.

A new thermally stable organoclay were then prepared through the modification of sodium montmorillonite with BAOB. An X-ray diffraction study confirmed the intercalation of organic surfactant within the silicate layers. SEM images showed that some significant changes occurred on the surface of BAOB-modified organoclay with respect to Na-MMT, including a decrease in hydrophilicity. Furthermore, the high thermal stability of BAOB avoids pyrolysis during thermal imidization of poly(amic acid) intermediate. The preparation and characterization of new PI/clay nanocomposite materials with different contents of BAOB-modified organoclay and PI **(7)** have also been investigated. PCNs 1-5% were prepared from the thermal imidization of a BAOB-modified organoclay dispersion in a poly(amic acid) solution obtained from BAOB and ODPA. WXRD patterns showed that exfoliated nanocomposite may be obtained with the organoclay content of 1%, but at higher clay loadings intercalated structure is significant. TGA and DSC measurements showed that T_g increases with increasing organoclay content loading to 3%, and then decrease thereafter. SEM images showed that the surface roughness of the film obtained from PCNs 1% is lower than that of the virgin polyimide.

Acknowledgement

The Graduate Council of the University of Mohaghegh Ardabili (Iran) is gratefully acknowledged for their financial support.

References

1. Liaw, D.-J.; Liaw, B.-Y. *Macromol. Chem. Phys.* **1998**, *199*, 1473-1478.
2. Imai, Y.; Itoya, K.; Kanamaru, M.; Kakimoto, M.-A. *J. Polym. Sci. Part A: Polym. Chem.* **2002**, *40*, 1790-1795.
3. Matsumoto, N.; Hiruma, H.; Nagaoka, S.; Fujiyama, K.; Kaneko, A.; Kawakami, H. *Polym. Adv. Technol.* **2008**, *19*, 1002-1008.
4. Meador, M. A. B.; Malow, E. J.; Silva, R.; Wright, S.; Quade, D.; Vivod, S. L.; Guo, H.; Guo, J.; Cakmak, M. *ACS Appl. Mater. Interfacec* **2012**, *4*, 536-544.
5. Wu, W.; Wang, K.; Zhan, M.-S. *Ind. Eng. Chem. Res.* **2012**, *51*, 12821-12826.
6. Chou, W.-Y.; Chang, M.-H.; Cheng, H.-L.; Lee, Y.-C.; Chang, C.-C.; Sheu, H.-S. *J. Phys. Chem. C.* **2012**, *116*, 8619-8626.
7. Ribeiro, C. P.; Freeman, B. D.; Kalika, D. S.; Kalakkunnath, S. *J. Membr. Sci.* **2012**, *390-391*, 182-193.
8. Yoonessi, M.; Shi, Y.; Scheiman, D. A.; Lebron-Colon, M.; Tigelaar, D. M.; Weiss, R. A.; Meador, M. A. *ACS Nano* **2012**, *6*, 7644-7655.
9. Battirola, L. C.; Gasparotto, L. H. S.; Rodrigues-Filho, U. P.; Tremiliosi-Filho, G. *Membranes* **2012**, *2*, 430-439.
10. Gong, G.; Wu, J.; Liu, J.; Sun, N.; Zhao, Y.; Jiang, L. *J. Mater. Chem*. **2012**, *22*, 8257-8262.
11. Chu, S.; Wang, Y.; Guo, Y.; Zhou, P.; Yu, H.; Luo, L.; Kong, F.; Zou, Z. *J. Mater. Chem*. **2012**, *22*, 15519-15521.
12. Mansoori, Y.; Fathollahi, K.; Reza, Z. M.; Imanzadeh, G. *Polym. Comps.* **2011**, *32*, 1862-1873.
13. Mansoori, Y.; Sanaei, S.; Zamanloo, M.-R.; Imanzadeh, G.; Atghia, S. *Bull. Mater. Sci.* **2013**, *36*, 789-798.
14. Burnside, S. D.; Giannelis, E. P. *Chem. Mater*. **1995**, *7*, 1597-1600.
15. Vaia, R. A.; Vasudevan, S.; Krawiec, W.; Scanlon, L. G.; Giannelis, E. P. *Adv. Mater*. **1995**, *7*, 154-156.
16. Gilman, J. W.; Jackson, C. L.; Morgan, A. B.; Harris, R.; Manias, E.; Giannelis, E. P.; Wuthenow, M.; Hilton, D.; Phillips, S. H. *Chem. Mater*. **2000**, *12*, 1866-1873.
17. Yeh, J.-M.; Liou, S.-J.; Chang, Y.-W. *J. Appl. Polym. Sci.* **2004**, *91*, 3489-3496.
18. Long, B.; Wang, C.-A.; Lin, W.; Huang, Y.; Sun, J. *Compos. Sci. Technol.* **2007**, *67*, 2770-2774.
19. hong, Y.; Janes, D.; Zheng, Y.; Hetzer, M.; De Kee, D. *Polym. Eng. Sci.* **2007**, *47*, 1101-1107.
20. Mansoori, Y.; Atghia, S. V.; Zamanloo, M. R.; Imanzadeh, G.; Sirousazar, M. *Eur. Polym. J.* **2010**, *46*, 1844-1853.
21. Mansoori, Y.; Atghia, S. V.; Sanaei, S. S.; Zamanloo, M. R.; Gh, I. *Macromol. Res*. **2010**, *18*, 1174-1181.
22. Yeum, J. H. *Polym-Plast. Technol. Eng.* **2011**, *50*, 1149-1154.
23. Sinha Ray, S.; Okamoto, M. *Prog. Polym. Sci*. **2003**, *28*, 1539-1641.
24. Ju, C. H.; Kim, J.-C.; Chang, J.-H. *J. Appl. Polym. Sci.* **2007**, *106*, 4192-4201.
25. Wang, H.-W.; Dong, R.-X.; Liu, C.-L.; Chang, H.-Y. *J. Appl. Polym. Sci.* **2007**, *104*, 318-324.
26. Yudin, V. E.; Otaigbe, J. U.; Gladchenko, S.; Olson, B. G.; Nazarenko, S.; Korytkova, E. N.; Gusarov, V. V. *Polymer* **2007**, *48*, 1306-1315.
27. Huang, C.-C.; Jang, G.-W.; Chang, K.-C.; Hung, W.-I.; Yeh, J.-M. *Polym. Intl.* **2008**, *57*, 605-611.
28. Voevodin, A. A.; O'Neill, J. P.; Zabinski, J. S. *Surf. Coat. Technol.* **1999**, *116-119*, 36-45.
29. Ringwald, S. C.; Pemberton, J. E. *Enviro. Sci. Technol.* **1999**, *34*, 259-265.
30. Yokoyama, R.; Suzuki, S.; Shirai, K.; Yamauchi, T.; Tsubokawa, N.; Tsuchimochi, M. *Eur. Polym. J.* **2006**, *42*, 3221-3229.
31. Liaw, D.-J.; Liaw, B.-Y.; Li, L.-J.; Sillion, B.; Mercier, R.; Thiria, R.; Sekiguchi, H. *Chem. Mater*. **1998**, *10*, 734-739.

32. Yeh, J.-M.; Chen, C.-L.; Kuo, T.-H.; Su, W.-F.; Huang, H.-Y.; Liaw, D.-J.; Lu, H.-Y.; Liu, C.-F.; Yu, Y.-H. *J. Appl. Polym. Sci.* **2004**, *92*, 1072-1079.
33. Liang, Z.-M.; Yin, J.; Xu, H.-J. *Polymer* **2003**, *44*, 1391-1399.
34. Chen, C.; Langat, J.; Raghavan, D. *Polym. Adv. Technol.* **2012**, *23*, 1287-1296.
35. Yousfi, M.; Soulestin, J.; Vergnes, B.; Lacrampe, M. F.; Krawczak, P. *J. Appl. Polym. Sci.* **2013**, *128*, 2766-2778.
36. Sheng, F.; Tang, X.-Z.; Zhang, S.; Ding, X.; Yu, Z.-Z.; Qiu, Z. *Polym. Adv. Technol.* **2012**, *23*, 137-142.
37. Abdallah, W.; Yilmazer, U. *J. Appl. Polym. Sci.* **2013**, *127*, 772-783.
38. Tyan, H.-L.; Wei, K.-H.; Hsieh, T.-E. *J. Polym. Sci. Part B: Polym. Phys*. **2000**, *38*, 2873-2878.
39. Ding, J.; Day, M.; Robertson, G.; Roovers, J. *Macromolecules* **2002**, *35*, 3474-3483.
40. Souza, F. G.; Sena, M. E.; Soares, B. G. *J. Appl. Polym. Sci.* **2004**, *93*, 1631-1637.
41. Kizhnyaev, V. N.; Pokatilov, A. F.; Vereshchagin, L. I.; Adamova, L. V.; Safronov, A. P.; Smirnov, A. I. *Russ. J. Appl. Chem.* **2006**, *79*, 1167-1173.
42. Chiang, P.-C.; Whang, W.-T. *Polymer* **2003**, *44*, 2249-2254.
43. Mansoori, Y.; Shah Sanaei, S.; Atghia, S. V.; Zamanloo, M. R.; Imanzadeh, G. *Chin. J. Polym. Sci.* **2011**, *29*, 699-711.
44. Mansoori, Y.; Kohi-Zargar, B.; Shekaari, H.; Zamanloo, M. R.; Imanzadeh, G. *Polym. Bull*. **2012**, *68*, 113-139.
45. Yagoub Mansoori; Somayeh Shah Sanaei; Mohammad-Reza Zamanloo; Gholamhassan Imanzadeh; Atghia, S. V. *Bull. Mater. Sci*. **2013**, *36*, 789-798.
46. Palekar, V. S.; Damle, A. J.; Shukla, S. R. *Eur. J Med. Chem.* **2009**, *44*, 5112-5116.
47. Wang S.-F., Lin M.-L., Shieh Y.-N., Wang Y.-R., Wang S.-J., *Ceram. Intl*. **2007**, *33*, 681-685.
48. Gu, A.; Kuo, S.-W.; Chang, F.-C. *J. Appl. Polym. Sci.* **2001**, *79*, 1902-1910.
49. Le, N. L.; Wang, Y.; Chung, T.-S. *J. Membr. Sci.* **2012**, *415-416*, 109-121.
50. Zidelkheir, B.; Abdelgoad, M. *J. Therm. Anal. Calorim.* **2008**, *94*, 181-187.
51. Delozier, D. M.; Orwoll, R. A.; Cahoon, J. F.; Johnston, N. J.; Smith Jr, J. G.; Connell, J. W. *Polymer* **2002**, *43*, 813-822.
52. Santiago, F.; Mucientes, A. E.; Osorio, M.; Rivera, C. *Eur Polym. J.* **2007**, *43*, 1-9.